Journal of Zhejiang University-SCIENCE A (Applied Physics & Engineering)
ISSN 1673-565X (Print); ISSN 1862-1775 (Online)
www.jzus.zju.edu.cn; www.springerlink.com
E-mail: jzus@zju.edu.cn

Non-monotonic piezocone dissipation curves of backfills in a soil-bentonite slurry trench cutoff wall*

Yu-chao LI[1], Xing TONG[1], Yun CHEN[2], Han KE[1], Yun-min CHEN[†‡1], Yi-duo WEN[1], Qian PAN[3]

[1]*MOE Key Laboratory of Soft Soils and Geoenvironmental Engineering, Zhejiang University, Hangzhou 310058, China*

[2]*Architectural Design and Research Institute of Zhejiang University Co., Ltd., Hangzhou 310028, China*

[3]*College of Civil Engineering and Architecture, Zhejiang University of Water Resources and Electric Power, Hangzhou 310018, China*

[†]E-mail: chenyunmin@zju.edu.cn

Received Feb. 22, 2017; Revision accepted July 28, 2017; Crosschecked Mar. 7, 2018

Abstract: Pore pressure dissipation during piezocone testing provides a unique tool for estimating the hydraulic properties of in-situ backfills in soil-bentonite (SB) slurry trench cutoff walls. Six tests were performed in an SB slurry trench cutoff wall located in Jiangsu Province, China. The pore pressure dissipation curves obtained are non-monotonic, which, as far as the authors are aware, is reported for the first time in SB cutoff walls. The non-monotonic dissipation curves are attributed to the redistribution of excess pore pressures between the base soil clods and the rest of the backfill around the cone. Four existing interpretation methods are adopted to analyze the measured non-monotonic piezocone dissipation curves. The horizontal coefficients of consolidation (c_h) of the backfills obtained by three methods are close to each other and in agreement with the results of fixed-ring consolidometer tests, while the other method gives a high overestimate. The hydraulic conductivities (k_h) of the backfills are also estimated by four methods, three based on dissipation test results and one based on piezocone penetration data. k_h estimated by consolidation theory are close to the results of flexible wall permeameter tests. Two empirical expressions for dissipation tests give relatively low k_h, but the method based on penetration gives k_h much larger than the laboratory test results.

Key words: Piezocone; Dissipation test; Soil-bentonite cutoff wall; Coefficient of consolidation; Hydraulic conductivity
https://doi.org/10.1631/jzus.A1700097 **CLC number:** TU45

1 Introduction

Soil-bentonite (SB) slurry trench cutoff walls have been widely employed in the United States to control seepage as groundwater retaining structures and prevent pollutant diffusion from contaminated lands. Achieving a low hydraulic conductivity (k_h) of the SB backfill is a critical concern in the design of cutoff walls, and typically $k_h \leq 10^{-7}$ cm/s is specified. Cone penetration testing (CPT) which is widely used for classifying soils and evaluating soil properties (Karakouzian et al., 2003; Elsworth and Lee, 2005; Cai et al., 2011; Bol, 2013; Wang et al., 2013) has also been often applied on the SB cutoff walls to check the continuity and strength of the backfill material (Jones et al., 2007; Ryan and Spaulding, 2008; Ruffing and Evans, 2010; Ruffing et al., 2015). Sometimes, the CPT with a pore-pressure transducer (CPTU) or piezocone (Baligh et al., 1981) has been used to measure hydraulic properties such as the coefficient of consolidation (c_h) and the hydraulic conductivity (k_h) of the SB, by interpreting the dissipation curves of excess pore pressure in the soil surrounding the cone after halting the penetration at a desired depth (Britton et al., 2004; Bennert et al., 2005).

‡ Corresponding author

* Project supported by the National Natural Science Foundation of China (No. 41672284) and the Science Technology Planning Project of Zhejiang Province (No. 2015C03021), China

ORCID: Yu-chao LI, https://orcid.org/0000-0002-3636-5007

Excess pore pressure induced by the penetration of the cone in the soil results from a combination of the changes in the octahedral normal stress and the shear stress (Teh and Houlsby, 1991; Burns and Mayne, 1998). Cavity-expansion theory and modified Cam-Clay model can be used to represent the generated excess pore pressure due to the changes of octahedral normal and shear stresses, respectively (Burns and Mayne, 1998, 2002; Chang et al., 2001; Chai et al., 2012, 2016). Monotonically decreasing pore pressures were usually measured in dissipation tests performed in soft, fine-grained silts and clays, while non-monotonic pore pressure dissipation curves with a temporary increase followed by a decrease were commonly recorded in overconsolidated clays or dense sandy soils (Lunne et al., 1986; Burns and Mayne, 1998, 2002; Sully et al., 1999; Imre et al., 2010; Chai et al., 2012; Ha et al., 2014), if a cone with the pore-pressure filter located immediately behind the tip at the shoulder is used. Several possible reasons have been suggested for non-monotonic dissipation behavior: (1) the effect of shear induced dilatancy (Coop and Wroth, 1989; Burns and Mayne, 1998; Chai et al., 2012); (2) volumetric expansion by a partial unloading effect when a soil element moves from the face to the shoulder of a cone (Teh and Houlsby, 1991; Chai et al., 2012); (3) redistribution of excess pore pressure from the face to the shoulder locations of the cone (Davidson, 1985; Sully et al., 1999; Colreavy et al., 2016); (4) poor saturation of the filter element (Burns and Mayne, 1998; Sully et al., 1999).

An interpretation method for the monotonic dissipation curves has been proposed to evaluate c_h (Teh and Houlsby, 1991). However, this method cannot be directly applied to non-monotonic dissipation curves. There are, however, several analytical, numerical, and empirical methods for interpreting non-monotonic dissipation curves (Burns and Mayne, 1998, 2002; Sully et al., 1999; Imre et al., 2010; Chai et al., 2012; Ansari et al., 2014; Ha et al., 2014; Mahmoodzadeh et al., 2014), and among them the methods proposed by Sully et al. (1999), Chai et al. (2012), and Ha et al. (2014) are relatively simple and applicable for engineering.

The hydraulic conductivity k_h of the soil can be estimated from c_h through consolidation theory (Terzaghi et al., 1996) or empirical formulas (Baligh and Levadoux, 1980; Parez and Fauriel, 1988; Cai et al., 2007), based on the pore pressure dissipation test. Since the dissipation test is time-consuming, especially for soft clay, Elsworth and Lee (2005, 2007) proposed a semi-rigorous approach, with no need of a dissipation test. Chai et al. (2011) and Shen et al. (2015) improved this kind of method and extended its application range.

In this paper, six sets of CPTU tests and dissipation tests were conducted in an SB slurry trench cutoff wall in Jiangsu Province, which is the first SB cutoff wall in China. The reasons for the measured non-monotonic curves are discussed. c_h of the in-situ backfill is evaluated by four existing interpretation methods for non-monotonic dissipation curves, and k_h of the backfill is also estimated by four methods. The validities of these methods are evaluated by comparing the calculation results with those of laboratory fixed-ring consolidometer tests and flexible wall permeameter tests, respectively.

2 Existing methods

2.1 Coefficients of consolidation (c_h)

Teh and Houlsby (1991) observed that monotonic pore pressure dissipation curves could be normalized using the following relation:

$$T^* = \frac{c_h t}{r^2 \sqrt{I_r}}, \tag{1}$$

where T^* is a modified time factor for a given probe geometry and porous element location, t is the measured time, r is the radius of the probe, and I_r is the rigidity index. This relation has been proved reasonable (Robertson et al., 1992; Abu-Farsakh and Nazzal, 2005) and is widely used to estimate c_h for soft, fine-grained silts and clays based on the time for 50% excess pore pressure dissipation (t_{50}):

$$c_h = \frac{T^* r^2 \sqrt{I_r}}{t_{50}}, \tag{2}$$

where T^* is 0.245 corresponding to t_{50} with the filter located at the shoulder of the cone. Although Eq. (2) cannot be directly applied to interpret non-monotonic dissipation curves, it provides a base for the methods

which attempt to modify this equation to make it compatible with the measured data of non-monotonic dissipation.

Sully et al. (1999) proposed two methods: the logarithm of time plot method and the square root of time plot method. The logarithm of time plot method corrects the non-monotonic dissipation curves into monotonic ones by shifting the origin of time to the point at which the maximum pore pressure (u_{max}) occurs, with all other times adjusted accordingly. The corrected time for 50% excess pore pressure dissipation (t_{50c}) can be found at (u_{max}+u_0)/2 (where u_0 is the hydrostatic pore pressure). The square root of time plot method back-extrapolates the dissipation curve to obtain the modified initial pore pressure (u_{im}) along the fitting straight line of the data after the time when the maximum pore pressure occurs (t_{umax}), and t_{50c} is then determined corresponding to (u_{im}+u_0)/2. Chai et al. (2012) proposed an empirical equation for correcting the time for 50% dissipation of u_{max} based on an uncoupled consolidation analysis:

$$t_{50c}=\frac{t_{50}}{1+18.5\left(\frac{t_{u\max}}{t_{50}}\right)^{0.67}\left(\frac{I_r}{200}\right)^{0.3}}, \tag{3}$$

where t_{50} is the observed time difference between u_{max} and (u_{max}+u_0)/2. For the three methods above (Sully et al., 1999; Chai et al., 2012), c_h can be obtained via Eq. (2), replacing t_{50} with t_{50c}. c_h for non-monotonic dissipation curves can also be obtained by the following equation proposed by Ha et al. (2014):

$$c_h=\frac{r^2(r_p/r)^{1.25}T_{50}^*}{t_{50i}}, \tag{4}$$

where r_p is the radius of the plastic zone, T_{50}^* is the modified time factor for 50% dissipation, t_{50i} is the time corresponding to (u_i+u_0)/2, and u_i is the measured initial pore pressure. r_p and T_{50}^* are calculated by the following expressions, respectively,

$$r_p=\left(0.24\frac{t_{50i}}{t_{u\max}}-0.86\right)r, \tag{5}$$

$$T_{50}^*=0.52\frac{u_{max}-u_0}{u_i-u_0}-0.25. \tag{6}$$

2.2 Hydraulic conductivities (k_h)

According to consolidation theory (Terzaghi et al., 1996), k_h can be estimated by the following relation according to c_h:

$$k_h=\frac{c_h\gamma_w}{E_s}, \tag{7}$$

where γ_w is the unit weight of water and E_s is the constrained modulus. Baligh and Levadoux (1980) proposed the following expression to estimate k_h based on c_h:

$$k_h=\frac{\gamma_w}{2.3\sigma'_{v0}}R_Rc_h, \tag{8}$$

where R_R represents the recompression ratio with a range of 0.005<R_R<0.02 recommended by Baligh and Levadoux (1980), and σ'_{v0} is the initial vertical effective stress. k_h can also be estimated though the empirical equation based on the 50% dissipation time t_{50} in the pore pressure dissipation test (Parez and Fauriel, 1988; Cai et al., 2007):

$$k_h=\left(251t_{50}\right)^{-1.25}, \tag{9}$$

where k_h is in cm/s and t_{50} is in s.

Elsworth and Lee (2005, 2007) proposed a semi-rigorous approach based on dislocation analysis, Darcy's law, and a spherical flow assumption. They derived an explicit equation as follows:

$$k_h=\frac{K_DUr\gamma_w}{4\sigma'_{v0}}, \tag{10}$$

where K_D is a dimensionless hydraulic conductivity index and U is the rate of cone penetration. However, Elsworth and Lee's method is applicable only for partially drained conditions, and Chai et al. (2011) presented a modified approach to estimate the hydraulic conductivity of soil based on a half spherical flow assumption, and extended the application range of Elsworth and Lee's approach from sandy soil to other soil types. Shen et al. (2015) additionally considered the influence of cone tip angles and soil property, and a half ellipsoid flow surface was assumed. For the specified piezocone with a tip angle α=60°, the expression for k_h could be written as

$$k_{\mathrm{h}}=\frac{1}{2.976\beta \mathrm{e}^{0.076\beta}}\cdot\frac{K_{\mathrm{D}}Ur\gamma_{\mathrm{w}}}{\sigma'_{\mathrm{v0}}}, \tag{11}$$

where β is a parameter indicating soil property and β=0.4 for clay, β=0.32 for silt, and β=0.15 for sand. K_{D} can be determined as

$$\begin{cases} K_{\mathrm{D}}=\dfrac{1}{B_{\mathrm{q}}Q_{\mathrm{t}}}, & B_{\mathrm{q}}Q_{\mathrm{t}}<0.45, \\ K_{\mathrm{D}}=\dfrac{0.044}{(B_{\mathrm{q}}Q_{\mathrm{t}})^{4.91}}, & B_{\mathrm{q}}Q_{\mathrm{t}}\geq 0.45, \end{cases} \tag{12}$$

where B_{q} and Q_{t} are the dimensionless pore water pressure ratio and dimensionless tip resistance, respectively, defined as (Wroth, 1984):

$$B_{\mathrm{q}}=\frac{u_2-u_0}{q_{\mathrm{t}}-\sigma_{\mathrm{v0}}}, \tag{13}$$

$$Q_{\mathrm{t}}=\frac{q_{\mathrm{t}}-\sigma_{\mathrm{v0}}}{\sigma'_{\mathrm{v0}}}, \tag{14}$$

where q_{t} is the total cone tip resistance and σ_{v0} is the initial total vertical stress.

3 Site condition and material properties

As a full-scale test, a soil-bentonite slurry trench cutoff wall with a length of 15 m, a width of 0.6 m, and a depth of 10 m (Fig. 1), was built at a municipal solid waste landfill in Jingjiang, Jiangsu Province in 2014. The investigation of stratigraphy showed that there were basically five layers within 16 m of depth at the site, and the geotechnical properties of each soil layer are presented in Table 1.

It is noted that the wall was not keyed into the impervious layer, since the primary aim of the test was to study the construction technology and consolidation behavior of the SB cutoff wall. The groundwater table is about 1.5 m below the ground surface.

The lean clay within 0.5–2.2 m was selected as the base soil of SB backfill due to its high fines content (72%) for achieving low-permeability backfill. Bentonite from Wyoming, USA with a liquid limit (LL) of 200.8 and a plastic index (PI) of 161.0 was used, and was classified as fat clay (CH) according to ASTM standard D2487-11 (ASTM, 2011b). Other properties of the bentonite are listed in Table 2. The grain-size distributions for both base soil and bentonite are shown in Fig. 2.

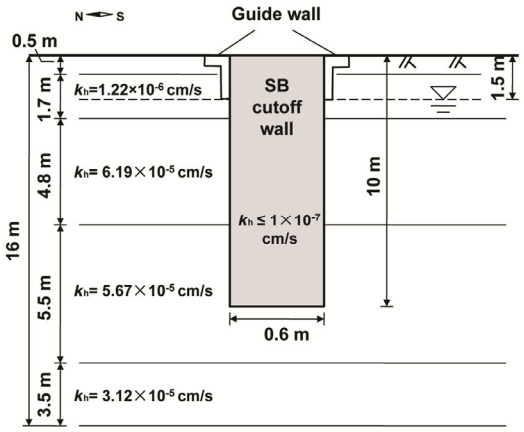

Fig. 1 Cross-section of SB slurry trench cutoff wall in layered soils

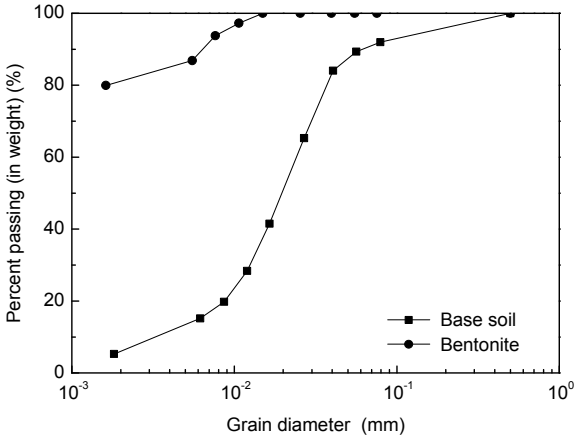

Fig. 2 Grain size distributions of bentonite and base soil

4 Laboratory tests

The bentonite content of the SB backfill was determined as 5% by dry weight, and the water content of the SB backfill corresponding to a slump of 125 mm was 51% based on standard slump tests (Fig. 3). The hydraulic properties of the backfill, that is the coefficient of consolidation (c_{h}) and the hydraulic conductivity (k_{h}), were estimated by the fixed-ring consolidometer test and the flexible wall permeameter test, respectively.

Table 1 Properties of soils at the test site

Depth (m)	Classification*	G_s	LL (%)	PI (%)	E_s (MPa)	c (kPa)	φ (°)	k_h (cm/s)
0–0.5	Miscellaneous fill	–	–	–	–	–	–	–
0.5–2.2	Lean clay	2.72	36.1	12.6	7.6	10.7	19.3	1.22×10^{-6}
2.2–7	Lean clay	2.69	37.6	7.8	5.6	5.8	21.4	6.19×10^{-5}
7–12.5	Silty clay	2.68	33.6	5.8	9.1	4.0	26.6	5.67×10^{-5}
12.5–16	Lean clay	2.69	34.4	7.9	7.7	4.9	23.9	3.12×10^{-5}

* According to unified soil classification system (ASTM, 2011b). G_s: specific gravity; c: cohesion; φ: internal frictional angle

Table 2 Properties of bentonite

Property		Value
Specific gravity, G_s		2.50
Content of montmorillonite (%)		71.4
Liquid limit, LL (%)		200.8
Plasticity index, PI (%)		161.0
Swelling index (ml/(2 g))		58
Specific surface (m^2/g)		52.3
Cation exchange capacity, CEC (mmol/(100 g))		76.49
Exchangeable metal ions (mmol/(100 g))	Na^+	47.40
	K^+	0.03
	Ca^{2+}	12.82
	Mg^{2+}	5.42

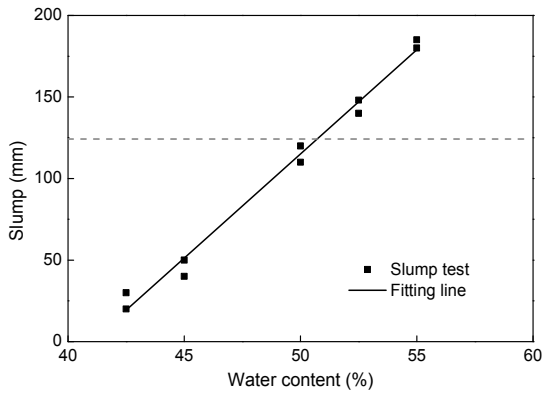

Fig. 3 Slump test result of soil-bentonite

4.1 Coefficient of consolidation (c_h)

The fixed-ring consolidometer tests on three samples were performed in accordance with ASTM D2435-11 (ASTM, 2011a). The samples were 61.8 mm in diameter and 20 mm in height. The load was started at 3.125 kPa and increased with a load increment ratio of 1, and the maximum loads were 800 kPa for two of the three samples and 100 kPa for the other one. For each load increment, the deformations of the samples were recorded at specific time intervals, and the maximum duration of each load increment was 24 h. According to the time-deformation relation, c_h under each load can be determined using the square root of time method. The variations of c_h for three samples with load pressures are shown in Fig. 4.

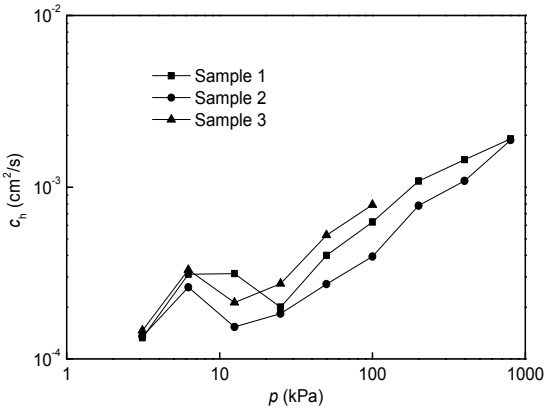

Fig. 4 Relationship between coefficient of consolidation c_h and consolidation stress p

4.2 Hydraulic conductivity (k_h)

The hydraulic conductivities of the SB backfill samples under 20 kPa, 40 kPa, and 80 kPa of effective consolidation stress were measured via a flexible wall permeameter, in accordance with ASTM D5084-10 (ASTM, 2010). Three parallel tests were performed under each consolidation pressure, and all the samples were initially 71.1 mm in diameter and 100 mm in height before consolidation. An acrylic cylinder was used to support the sample before application of cell pressure, and was left in place during the test (Baxter, 2000; Malusis et al., 2009). After 24 h of consolidation under each pressure, the sample was permeated under a constant head, and the quantities of inflow and outflow were measured and recorded periodically. The hydraulic conductivity was calculated via the following equation:

$$k_{\mathrm{h}}=\frac{\Delta Q\cdot L}{A\cdot\Delta h\cdot\Delta t},\tag{15}$$

where ΔQ is the quantity of flow for given time interval Δt, taken as the average of inflow and outflow; L is the length of sample; A is the cross-sectional area of the sample; Δh is the average head loss across the sample. The relation between the hydraulic conductivity of the backfill and the effective consolidation pressure is shown in Fig. 5. As can be seen in the figure, all the measured hydraulic conductivities are less than 1×10^{-7} cm/s, which indicates that the backfill with a bentonite content of 5% satisfies the design criterion if the effective consolidation pressure is not less than 20 kPa.

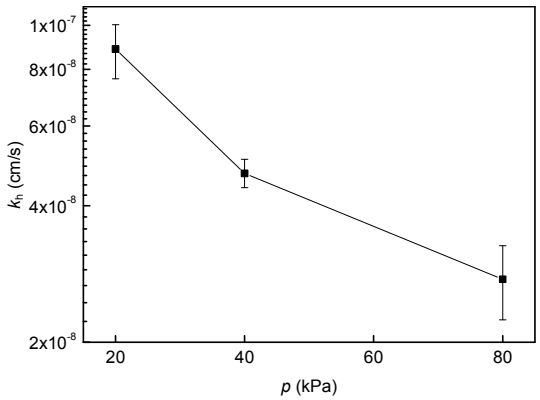

Fig. 5 Relationship between hydraulic conductivity k_{h} and consolidation stress p

5 SB cutoff wall construction

Before the construction of the SB slurry trench cutoff wall, the bentonite slurry for making backfills and maintaining trench stability was prepared by mixing bentonite with water using a flash mixer, according to a mass ratio of 1:19. Then the bentonite slurry was set aside in a low speed circulation pond for at least 24 h before use. The base soil was excavated and piled in advance. Considering the 27.6% water content of the excavated base soil, the SB backfill was made by mixing bentonite slurry, excavated base soil, and dry bentonite with a mass ratio of 6.7:32.2:1.0 in a concrete blender in the field.

Concrete guide walls (70 cm in height and 20 cm in thickness) were installed to prevent shallow collapse during the trench excavation. The trench was excavated by a clamshell bucket without a kelly bar, digging primary and secondary panels, with bentonite slurry pumped into the trench to maintain its stability. The mixed SB was dumped into the trench via a tremie pipe, which was keyed into the placed backfill to avoid segregation, to form a low-permeability barrier.

6 Piezocone penetration and dissipation tests

Piezocone tests were performed 15 months after the construction of the SB cutoff wall. The piezocone has a cross-section area of 10 cm^2 (60° cone angle and 150 cm^2 sleeve area) and a 5-mm filter element at the shoulder of the cone. Much attention was paid to the saturation of the porous filter and the piezocone tip with de-aired glycerin (Cai et al., 2012; Liu et al., 2014) as poor saturation affects the accuracy of pore pressure measurements. The piezocone was jacked steadily into the SB cutoff wall at a rate of 2.0 cm/s, with the resistance, sleeve friction, and pore pressure measured during penetration. The piezocone was held in position and the pore pressure dissipation test was conducted by monitoring the dissipating process of the pore pressure when the required depth was reached.

Six piezocone penetration tests named as CPTU 1, 2, 3, 4, 5, and 6 were performed in the SB cutoff wall, and their locations are shown in Fig. 6. All the test boreholes were arrayed along the centerline, and the minimum distance between two adjacent boreholes was 1 m. One of the piezocone penetration results, that is CPTU 4, with profiles of corrected tip resistance (q_{t}), sleeve friction (f_{s}), pore pressure (u_2), and friction ratio (R_{f}), is shown in Fig. 7.

As shown in Fig. 7, the q_{t}, f_{s}, and R_{f} of the SB backfill above groundwater table are higher than those below the groundwater table. Below 2 m of the depth, q_{t} and u_2 increase while f_{s} and R_{f} decrease with depth, in general. However, it is interesting to find that the peaks in the curves of q_{t} and f_{s} and the valleys in the curve of u_2 occur simultaneously (e.g. the circles at 4 m in Fig. 7). At a depth near 10 m, both q_{t} and f_{s} increase sharply, since the piezocone reaches the bottom of the cutoff wall.

Among these test boreholes, six dissipation tests, named as T1, T2, T3, T4, T5, and T6, were performed at various depths (2 m, 4 m, 6 m, 5 m, 7 m, 9 m), and the dissipation curves are plotted in Fig. 8. All the tests were stopped with over 1200 s of pore-pressure dissipation, and three tests were performed for more than 10000 s. It can be found that these measured dissipation curves are non-monotonic.

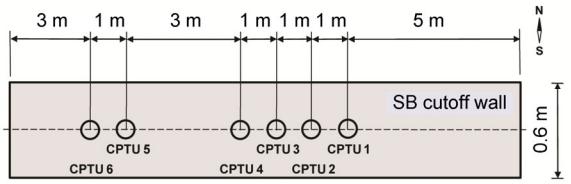

Fig. 6 Plane layout of CPTU boreholes

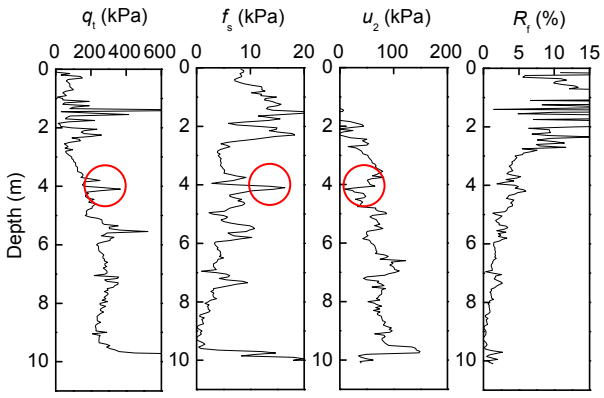

Fig. 7 Piezocone penetration results of CPTU 4 in SB cutoff wall

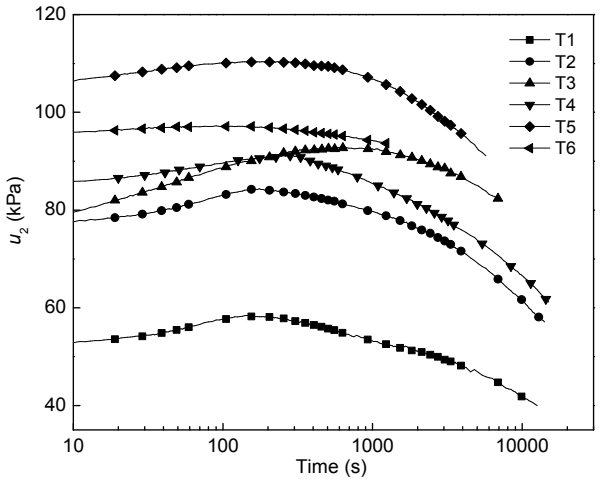

Fig. 8 Pore pressure dissipation curves of six piezocone dissipation tests in SB cutoff wall

7 Discussion

7.1 Mechanism of non-monotonic dissipation

The non-monotonic dissipation curves usually occurred in overconsolidated clays or dense sandy soils, but the soil-bentonite backfill is commonly considered as a normally consolidated soft soil because it is formed by mixing soil and bentonite slurry, having a high water content and low permeability, and is then consolidated under vertical stress (less than overburden due to sidewall friction) and horizontal stress (exerted by the surrounding soil).

However, unlike the laboratory sample which is mixed well, the backfill mixed in field conditions often has lower uniformity, especially when the base soil is cohesive. It means there are a lot of small clods of base soil packed in the backfill during mixing. If the diameters of the clods are close to or larger than the piezocone, they will have an influence on the measured mechanical and hydraulic properties. One example is the increasing q_t and f_s as well as the decreasing u_2 when the cone moves through the regions containing large clods (Fig. 7), since the clod has higher stiffness and permeability than the rest of the backfill that consists of the finer soil particles and the bentonite slurry.

The mechanism of non-monotonic dissipation curves can also be explained by the influence of clods. When the piezocone is penetrated downwards, the cone will push the clods, and the clods will also push the rest of the backfill. Due to the lower hydraulic conductivity of the backfill compared with the clod of base soil, the excess pore pressure generated in the backfills which are relatively far from the cone will be greater than that generated in the clods which are close to the cone. Then drainage will occur under the gradient between the backfill and the clods, and that is why the pore pressure near the cone will increase first. This mechanism is similar to the redistribution of excess pore pressure in overconsolidated soil during dissipation tests (Sully et al., 1999; Chai et al., 2014). Because of the low hydraulic conductivity of the backfill, the average time for reaching the maximum pore pressure $t_{u\max}$ is 245 s in this paper, much greater than $t_{u\max}$ presented by Ha et al. (2014). For backfills with a base soil of sand or silt, this effect would be weak as their uniformity is better, and monotonically decreasing pore pressures will be measured as in

normally consolidated soil (Bennert et al., 2005; Takai et al., 2013).

7.2 Validation of calculation methods

Four existing methods (Sully et al., 1999; Chai et al., 2012; Ha et al., 2014) are adopted to interpret the non-monotonic dissipation curves presented in Fig. 8, and the t_{50c} and c_h obtained are given in Table 3. It is noted that only T4 among the six piezocone dissipation tests was performed with more than 50% dissipation of the excess pore pressure as the SB backfills had extremely low hydraulic conductivity. For the other dissipation tests, the time for 50% dissipation of excess pore pressure is determined by extrapolating the straight-line portion in the square root of time plot similar to the Taylor method (Sully et al., 1999). The rigidity index I_r for SB backfill was determined as 88.0 by laboratory undrained triaxial compression tests ($I_r=G_{50}/s_u$, G_{50} is the secant shear modulus at 50% of failure stress (Ha et al., 2014), and s_u is the undrained shear strength). The radius of the piezocone was 1.78 cm.

As c_h is inversely proportional to t_{50c} in Eq. (2), the logarithm of time plot method gives the lowest c_h among the first three methods. It is also found that the results obtained by the logarithm of time plot method are close to those obtained by the square root of time plot method. The values obtained by both methods are in good agreement with the fixed-ring consolidometer test results presented in Fig. 4 (that is, $c_h=1.5\times10^{-4}$–8.0×10^{-4} cm^2/s for 12.5 kPa≤p≤100 kPa). c_h given by Chai et al. (2012)'s method are slightly higher than those from Sully et al. (1999)'s two methods, and are about 1.5–2.2 times the results obtained by the logarithm of time plot method. Moreover, the method of Ha et al. (2014) gives much greater c_h, which are 2.7–13.6 times the results obtained by the logarithm of time plot method. This may be because r_p is overestimated for the SB backfills using Eq. (5), which was established by Ha et al. (2014) via sensitivity analysis.

k_h of the backfill is evaluated by Eqs. (7)–(9), based on the obtained t_{50c} and c_h using the logarithm of time plot method (Table 3, Sully et al. (1999)'s method I). E_s for the backfill considered in Eq. (7) can be obtained from fixed-ring consolidometer tests, and E_s=0.6 MPa was measured as an average value for 12.5 kPa≤p≤100 kPa. The R_R in Eq. (8) was not tested and R_R=0.01 is assumed to avoid great errors. σ'_{v0} is estimated with the modified "lateral squeezing" model proposed by Ruffing et al. (2010), in which the horizontal effective stress is considered as the major effective principal stress:

$$\sigma'_h = K_{am}\gamma'_s z = 10^{\left(\frac{2\Delta - BC_1}{BC_{c\varepsilon}}\right)}, \tag{16}$$

where K_{am} is the mobilized active earth pressure coefficient of the soil outside the trench (which is simplified as mid-dense sand) and is a function of the lateral displacement (Δ) (Ruffing et al., 2010); γ'_s is the effective unit weight of the soil outside the trench and is taken as 17.6 and 8.3 for the soil above and below the groundwater table, respectively; z is the calculation depth; B is the trench width and B=0.6 m; $C_{c\varepsilon}$ and C_1 are the modified compression index and the strain at a unit effective stress in a 1D consolidation test and were separately measured as 0.11 and −0.05 for the SB backfill. σ'_{v0} is then calculated by $\sigma'_{v0}=K_0\sigma'_h$ (Filz, 1996), where the at-rest earth pressure coefficient K_0=1−sinφ and the internal

Table 3 t_{50c}/t_{50i} and c_h of SB backfills evaluated by four existing interpretation methods

Test No.	Depth (m)	t_{umax} (s)	Sully et al. (1999)'s method I*		Sully et al. (1999)'s method II**		Chai et al. (2012)'s method		Ha et al. (2014)'s method	
			t_{50c} (min)	c_h (cm^2/s)	t_{50c} (min)	c_h (cm^2/s)	t_{50c} (min)	c_h (cm^2/s)	t_{50i} (min)	c_h (cm^2/s)
T1	2.0	150	377.8	3.2×10^{-4}	360.2	3.4×10^{-4}	251.6	4.8×10^{-4}	472.1	4.4×10^{-3}
T2	4.0	175	264.3	4.6×10^{-4}	238.9	5.1×10^{-4}	154.9	7.8×10^{-4}	328.3	3.2×10^{-3}
T3	6.0	593	420.3	2.9×10^{-4}	353.3	3.4×10^{-4}	193.5	6.3×10^{-4}	743.4	1.5×10^{-3}
T4	5.0	281	213.7	5.7×10^{-4}	179.1	6.8×10^{-4}	100.9	1.2×10^{-3}	241.6	1.5×10^{-3}
T5	7.0	185	178.6	6.8×10^{-4}	151.9	8.0×10^{-4}	91.4	1.3×10^{-3}	224.4	2.8×10^{-3}
T6	9.0	90	124.2	9.8×10^{-4}	110.0	1.1×10^{-3}	70.9	1.7×10^{-3}	152.6	6.1×10^{-3}

* Logarithm of time plot method; ** Square root of time plot method

frictional angle φ=30°. k_h obtained by the three methods are given in Table 4. In addition, k_h is estimated by Eq. (11) proposed by Shen et al. (2015), and β=0.4, U=2 cm/s are adopted for SB backfill. K_D=0.044/$(B_qQ_t)^{4.91}$ is used since B_qQ_t>0.45. For comparison, k_h obtained from the penetration data at the same depths with dissipation tests are also presented in Table 4.

As can be seen, the hydraulic conductivities obtained by Eq. (7) range from 4.8×10^{-8} to 1.6×10^{-7} cm/s, while k_h obtained by Eq. (8) range from 9.9×10^{-9} to 2.7×10^{-8} cm/s. Both of the ranges are close to that of the flexible wall permeameter test results (i.e. k_h=2.2×10^{-8}–1.0×10^{-7} cm/s for 20 kPa≤p ≤80 kPa, Fig. 5), but if the stress state is considered, the results given by Eq. (7) are more reasonable. Moreover, Eq. (9) gives much lower k_h compared to Eq. (8), which may cause an unconservative assessment of the hydraulic performance of SB cutoff walls. By contrast, Eq. (11) gives much greater k_h than the laboratory test results, which are about 1–3 orders of magnitude larger than those obtained by Eq. (7). Thus, the equation based on Terzaghi's consolidation theory is considered more appropriate for determining the hydraulic conductivity of the SB cutoff wall through a CPTU dissipation test, because it has a relatively definite mechanism and gives the closest result to the laboratory test. The other methods may be suitable for normal ground cases, but need development before being applied in the SB cutoff walls. Meanwhile, another key difficulty in the application of these methods is the determination of vertical effective stress. Although the SB cutoff wall has been widely employed in engineering for decades, the real stress state and consolidation mechanism in the wall have not been fully understood (Bennert et al., 2005; National Research Council, 2007; Li et al., 2015; Ruffing et al., 2015), and the modified lateral squeezing model (Ruffing et al., 2010) is used in this study.

8 Conclusions

Piezocone penetration and dissipation tests were performed to evaluate the hydraulic properties of the backfill of an SB slurry trench cutoff wall located in Jiangsu Province, China. The pore pressure dissipation curves obtained are non-monotonic, which are usually measured in overconsolidated clays. As far as the authors know they are now reported for the first time for SB cutoff walls. The measured initial increase of pore pressure perhaps results from the redistribution of excess pore pressure around the cone which is affected by the ununiformity of the backfill, and the duration for pore pressure increase depends on the hydraulic conductivity of the backfill. Four existing interpretation methods are adopted to analyze the measured non-monotonic piezocone dissipation curves. c_h obtained by the logarithm of time plot method and the square root of time plot method (Sully et al., 1999) are close and in good agreement with the results of fixed-ring consolidometer tests. The empirical equation proposed by Chai et al. (2012) gives slightly higher results. Ha et al. (2014)'s method gives much higher c_h compared with the other three methods. Similarly, four methods are used to estimate k_h of the backfill, three based on the results of piezocone dissipation tests and one based on penetration. The relation of consolidation theory gives k_h closest to the results of flexible wall permeameter tests, and the two empirical methods underestimate, while the method based on penetration overestimates, the k_h of the backfill.

Table 4 k_h estimated for SB backfills by four existing methods

Depth (m)	σ'_{v0} (kPa)	B_q	Q_t	k_h (cm/s)			
				Eq. (7)	Eq. (8)	Eq. (9)	Eq. (11)
2.0	6.31	0.22	30.47	5.4×10^{-8}	2.2×10^{-8}	3.6×10^{-9}	1.7×10^{-7}
4.0	10.70	0.26	16.98	7.7×10^{-8}	1.9×10^{-8}	5.6×10^{-9}	8.2×10^{-7}
5.0	11.69	0.39	10.32	9.5×10^{-8}	2.1×10^{-8}	7.3×10^{-9}	1.2×10^{-6}
6.0	12.68	0.12	19.44	4.8×10^{-8}	9.9×10^{-9}	3.1×10^{-9}	1.3×10^{-5}
7.0	13.67	0.20	15.51	1.1×10^{-7}	2.2×10^{-8}	9.2×10^{-9}	3.3×10^{-6}
9.0	15.64	0.09	12.71	1.6×10^{-7}	2.7×10^{-8}	1.4×10^{-8}	4.8×10^{-4}

References

Abu-Farsakh MY, Nazzal MD, 2005. Reliability of piezocone penetration test methods for estimating the coefficient of consolidation of cohesive soils. *Transportation Research Record: Journal of the Transportation Research Board*, 1913:62-76. https://doi.org/10.3141/1913-07

Ansari Y, Merifield R, Sheng D, 2014. A piezocone dissipation test interpretation method for hydraulic conductivity of soft clays. *Soils and Foundations*, 54(6):1104-1116. https://doi.org/10.1016/j.sandf.2014.11.006

ASTM (American Society for Testing and Materials), 2010. Standard Test Methods for Measurement of Hydraulic Conductivity of Saturated Porous Materials Using a Flexible Wall Permeameter, ASTM D5084-10. ASTM, West Conshohocken, USA.

ASTM (American Society for Testing and Materials), 2011a. Standard Test Methods for One-dimensional Consolidation Properties of Soils Using Incremental Loading, ASTM D2435-11. ASTM, West Conshohocken, USA.

ASTM (American Society for Testing and Materials), 2011b. Standard Practice for Classification of Soils for Engineering Purposes (Unified Soil Classification System), ASTM D2487-11. ASTM, West Conshohocken, USA.

Baligh MM, Levadoux JN, 1980. Pore Pressure Dissipation after Cone Penetration. Department of Civil Engineering, Massachusetts Institute of Technology, USA.

Baligh MM, Azzouz AS, Wissa AZE, et al., 1981. The piezocone penetrometer. Cone Penetration Testing and Experience: Proceedings of a Session Sponsored by the Geotechnical Engineering Division at the ASCE National Convention.

Baxter DY, 2000. Mechanical Behavior of Soil-bentonite Cutoff Walls. PhD Thesis, Virginia Polytechnical Institute and State University, Blacksburg, USA.

Bennert TA, Maher A, Jafari F, 2005. Piezocone evaluation of a shallow soil-bentonite slurry wall. Geo-Frontiers Congress, ASCE. https://doi.org/10.1061/40789(168)43

Bol E, 2013. The influence of pore pressure gradients in soil classification during piezocone penetration test. *Engineering Geology*, 157:69-78. https://doi.org/10.1016/j.enggeo.2013.01.016

Britton JP, Filz GM, Herring WE, 2004. Measuring the hydraulic conductivity of soil–bentonite backfill. *Journal of Geotechnical and Geoenvironmental Engineering*, 130(12):1250-1258. https://doi.org/10.1061/(ASCE)1090-0241(2004)130:12(1250)

Burns SE, Mayne PW, 1998. Monotonic and dilatory pore-pressure decay during piezocone tests in clay. *Canadian Geotechnical Journal*, 35(6):1063-1073. https://doi.org/10.1139/t98-062

Burns SE, Mayne PW, 2002. Analytical cavity expansion-critical state model for piezocone dissipation in fine-grained soils. *Soils and Foundations*, 42(2):131-137. https://doi.org/10.3208/sandf.42.2_131

Cai GJ, Liu SY, Tong LY, et al., 2007. Study on consolidation and permeability properties of Lianyungang marine clay based on piezocone penetration test. *Chinese Journal of Rock Mechanics and Engineering*, 26(4):846-852 (in Chinese).

Cai GJ, Liu SY, Puppala AJ, 2011. Comparison of CPT charts for soil classification using PCPT data: example from clay deposits in Jiangsu Province, China. *Engineering Geology*, 121(1-2):89-96. https://doi.org/10.1016/j.enggeo.2011.04.016

Cai GJ, Liu SY, Puppala AJ, 2012. Predictions of coefficient of consolidation from CPTU dissipation tests in Quaternary clays. *Bulletin of Engineering Geology and the Environment*, 71(2):337-350. https://doi.org/10.1007/s10064-011-0385-4

Chai JC, Agung PMA, Hino T, et al., 2011. Estimating hydraulic conductivity from piezocone soundings. *Géotechnique*, 61(8):699-708. https://doi.org/10.1680/geot.10.P.009

Chai JC, Sheng DC, Carter JP, et al., 2012. Coefficient of consolidation from non-standard piezocone dissipation curves. *Computers and Geotechnics*, 41(4):13-22. https://doi.org/10.1016/j.compgeo.2011.11.005

Chai JC, Hossain MJ, Carter J, et al., 2014. Cone penetration-induced pore pressure distribution and dissipation. *Computers and Geotechnics*, 57(4):105-113. https://doi.org/10.1016/j.compgeo.2014.01.008

Chai JC, Hossain MJ, Yuan DJ, et al., 2016. Pore pressures induced by piezocone penetration. *Canadian Geotechnical Journal*, 53(3):540-550. https://doi.org/10.1139/cgj-2015-0206

Chang MF, Teh CI, Cao LF, 2001. Undrained cavity expansion in modified Cam clay II: application to the interpretation of the piezocone test. *Géotechnique*, 51(4):335-350. https://doi.org/10.1680/geot.2001.51.4.335

Colreavy C, O'loughlin CD, Randolph MF, 2016. Estimating consolidation parameters from field piezoball tests. *Géotechnique*, 66(4):333-343. https://doi.org/10.1680/jgeot.15.P.106

Coop MR, Wroth CP, 1989. Field studies of an instrumented model pile in clay. *Géotechnique*, 39(4):679-696. https://doi.org/10.1680/geot.1989.39.4.679

Davidson JL, 1985. Pore Pressure Generated during Cone Penetration Testing in Heavily Overconsolidated Clays. In Discussion Session 2D: Field Instrumentation and Field Measurements. Proceedings of the 11th International Conference on Soil Mechanics and Found, 5:2699.

Elsworth D, Lee DS, 2005. Permeability determination from on-the-fly piezocone sounding. *Journal of Geotechnical and Geoenvironmental Engineering*, 131(5):643-653. https://doi.org/10.1061/(ASCE)1090-0241(2005)131:5(643)

Elsworth D, Lee DS, 2007. Limits in determining permeability

from on-the-fly UCPT sounding. *Géotechnique*, 57(8): 679-685.
https://doi.org/10.1680/geot.2007.57.8.679

Filz GM, 1996. Consolidation stresses in soil-bentonite backfilled trenches. 2nd International Congress on Environmental Geotechnics, p.497-502.

Ha TG, Jang IS, Choo YS, et al., 2014. Evaluation of coefficient of consolidation for dilatory dissipation in piezocone test in overconsolidated cohesive soils. *KSCE Journal of Civil Engineering*, 18(2):475-487.
https://doi.org/10.1007/s12205-014-0191-1

Imre E, Rozsa P, Bates L, et al., 2010. Evaluation of monotonic and non-monotonic dissipation test results. *Computers and Geotechnics*, 37(7-8):885-904.
https://doi.org/10.1016/j.compgeo.2010.07.008

Jones S, Spaulding C, Symth P, 2007. Design and construction of a deep soil-bentonite groundwater barrier wall at Newcastle, Australia. 10th Australian New Zealand Conference on Geomechanics Common Ground.

Karakouzian M, Avar BB, Hudyma N, et al., 2003. Field measurements of shear strength of an underconsolidated marine clay. *Engineering Geology*, 67(3-4):233-242.
https://doi.org/10.1016/S0013-7952(02)00182-5

Li YC, Cleall PJ, Wen YD, et al., 2015. Stresses in soil–bentonite slurry trench cut-off walls. *Géotechnique*, 65(10):843-850.
https://doi.org/10.1680/geot.14.P.219

Liu SY, Ju J, Cai GJ, et al., 2014. Stress history estimation method of underconsolidated soil by partial piezocone dissipation tests. *Marine Georesources and Geotechnology*, 32(4):368-378.
https://doi.org/10.1080/1064119X.2013.778376

Lunne T, Eidsmoen TE, Powell JJM, et al., 1986. Piezocone testing in overconsolidated clays. 39th Canadian Geotechnical Conference, p.209-218.

Mahmoodzadeh H, Randolph MF, Wang D, 2014. Numerical simulation of piezocone dissipation test in clays. *Géotechnique*, 64(8):657-666.
https://doi.org/10.1680/geot.14.P.011

Malusis MA, Barben EJ, Evans JC, 2009. Hydraulic conductivity and compressibility of soil-bentonite backfill amended with activated carbon. *Journal of Geotechnical and Geoenvironmental Engineering*, 135(5):664-672.
https://doi.org/10.1061/(ASCE)GT.1943-5606.0000041

National Research Council, 2007. Assessment of the Performance of Engineered Waste Containment Barriers. National Academies Press, Washington DC, USA.

Parez L, Fauriel R, 1988. Le piezocone ameliorations apportees a la reconnaissance de sols. *Revue Française de Géotechnique*, 44:13-27 (in French).

Robertson PK, Sully JP, Woeller DJ, et al., 1992. Estimating coefficient of consolidation from piezocone tests. *Canadian Geotechnical Journal*, 29(4):539-550.
https://doi.org/10.1139/t92-061

Ruffing DG, Evans JC, 2010. In situ evaluation of a shallow soil bentonite slurry trench cutoff wall. Proceedings of the 6th International Congress on Environmental Geotechnics, p.756-763.

Ruffing DG, Evans JC, Malusis MA, 2010. Prediction of earth pressures in soil-bentonite cutoff walls. GeoFlorida Conference, ASCE, p.2416-2425.
https://doi.org/10.1061/41095(365)245

Ruffing DG, Evans JC, Ryan CR, 2015. Strength and stress estimation in soil bentonite slurry trench cutoff walls using cone penetration test data. Proceedings of the International Foundations Congress and Equipment Expo, p.2567-2576.
https://doi.org/10.1061/9780784479087.238

Ryan CR, Spaulding CA, 2008. Strength and permeability of a deep soil bentonite slurry wall. GeoCongress: Geotechnics of Waste Management and Remediation, ASCE, p.644-651.
https://doi.org/10.1061/40970(309)81

Shen SL, Wang JP, Wu HN, et al., 2015. Evaluation of hydraulic conductivity for both marine and deltaic deposit based on piezocone test. *Ocean Engineering*, 110(A): 174-182.
https://doi.org/10.1016/j.oceaneng.2015.10.011

Sully JP, Robertson PK, Campanella RG, et al., 1999. An approach to evaluation of field CPTU dissipation data in overconsolidated fine-grained soils. *Canadian Geotechnical Journal*, 36(2):369-381.
https://doi.org/10.1139/t98-105

Takai A, Inui T, Katsumi T, et al., 2013. Hydraulic Barrier Performance of Soil Bentonite Mixture Cutoff Wall. International Symposium on Coupled Phenomena in Environmental Geotechnics, p.707-714.
https://doi.org/10.1201/b15004-96

Teh CI, Houlsby GT, 1991. An analytical study of the cone penetration test in clay. *Géotechnique*, 41(1):17-34.
https://doi.org/10.1680/geot.1991.41.1.17

Terzaghi K, Peck RB, Mesri G, 1996. Soil Mechanics in Engineering Practice. Wiley, New York, USA.

Wang JP, Xu YS, Ma L, et al., 2013. An approach to evaluate hydraulic conductivity of soil based on CPTU test. *Marine Georesources and Geotechnology*, 31(3):242-253.
https://doi.org/10.1080/1064119X.2012.676154

Wroth CP, 1984. The interpretation of in situ soil tests. *Géotechnique*, 34(4):449-489.
https://doi.org/10.1680/geot.1984.34.4.449

中文概要

题　目： 土-膨润土隔离墙孔压静力触探非单调消散曲线研究

目　的： 土-膨润土隔离墙的水力特性可通过孔压静力触

探试验进行评价。本文旨在研究土-膨润土隔离墙中孔压消散试验产生非单调孔压消散曲线的原因，并对现有计算固结系数与渗透系数的方法在土-膨润土隔离墙中的适用性进行分析。

创新点： 1. 首次在土-膨润土隔离墙中测得非单调的孔压消散曲线；2. 本文认为在土-膨润土隔离墙中测得非单调孔压消散曲线是由于探头贯入过程中在填料及其包裹的土块中产生的超孔压不一致引起的，并且由于填料的低渗透性，孔压上升的时间较长；3. 比较不同方法的分析结果，并推荐结果与实测相近的计算方法作为工程应用。

方　法： 1. 通过室内一维固结试验和柔性壁渗透试验，分别获得墙体材料的固结系数和渗透系数；2. 通过现场土-膨润土隔离墙的孔压静力触探试验与孔压消散试验，获得相应的力学参数与孔压消散曲线；3. 分别采用不同方法对墙体材料的固结系数和渗透系数进行计算，并将计算结果与室内试验结果进行比较。

结　论： 1. 填料的非均质性导致探头贯入过程中产生的超孔压存在重分布，这使得土-膨润土隔离墙中产生了非单调孔压消散曲线，并且由于填料的低渗透性，测得孔压上升的时间较长；2. 四种计算固结系数的方法中，有三种结果与室内一维固结试验结果相近，另一种结果则明显偏大；3. 四种计算渗透系数的方法中，基于太沙基固结理论的关系式得到的结果与室内柔壁渗透试验结果相近，另两种经验公式得到的结果偏小，而基于探头贯入数据计算的渗透系数则偏大。

关键词： 孔压静力触探；消散试验；土-膨润土隔离墙；固结系数；渗透系数